Hindawi
Advances in Materials Science and Engineering
Volume 2022, Article ID 7051650, 11 pages
https://doi.org/10.1155/2022/7051650

Research Article

Effect of Surface Roughness and Particle Size on Lubrication Mechanisms of SiO_2 Nanoparticles

Linghui Kong,[1] Lei Zhang ,[1] Yueyue Bao,[2] Dong Liu,[1] and Shutan Liu[1]

[1]*The Yellow River Institute of Hydraulic Research, The Yellow River Water Conservancy Commission, Zhengzhou 450003, China*
[2]*School of Materials Science and Engineering, University of Science and Technology, Beijing 100083, China*

Correspondence should be addressed to Lei Zhang; hkyzhanglei@163.com

Received 29 July 2022; Accepted 26 September 2022; Published 18 October 2022

Academic Editor: Zhigang Zang

In this study, a series of tribological tests were conducted on a pin-on-disc tester to study the lubrication mechanism of SiO_2 nanoparticles under different surface roughness considering various loads and velocities. For a comprehensive understanding of the mechanism of SiO_2 nanoparticles, base fluid was also employed as a contrast. Results show that the reductions of friction coefficients and wear scar widths increase with the decrease of surface roughness, due to the increase in rolling effect and self-repairing mechanism of SiO_2 nanoparticles. The lubrication mechanism of SiO_2 nanoparticles is the rolling effect when the height-diameter ratio (λ) is less than 6, and the self-repairing mechanism at λ of 6 and 10, whereas, there is no obvious difference by adding nanoparticles when λ is 20. When the height-diameter ratio is less than 6, surface wears show an increasing trend as the load increases due to the high hardness of nanoparticles, while it is the opposite at λ of 10 and 20 because of the self-repairing mechanism.

1. Introduction

With the vigorous development of nanotechnology, an increasing number of nanomaterials are widely used in the field of semiconductors, such as SiO_2 [1], TiO_2 [2], carbon nanotubes [3], quantum dots [4], and lead halide perovskite nanocrystals [5]. Graphene and MoS_2 and their derivatives are involved in active optoelectronics devices [6], catalysts [7, 8], spin-valleytronic [9], and biomedicine [10]. In recent years, the outstanding tribological properties of nanoparticles have also received wide attention in tribology due to their small size and high surface activity. Du et al. investigated the anti-wear and friction-reducing performance of graphene oxide-TiO_2 nanocomposite, which exhibited superior film-forming stability [11]. Xiong et al. [12] synthesized SiO_2-reinforced B–N-co-doped graphene oxide and found that the optimal tribological behavior was obtained when the concentration was 0.15 wt.%. Extensive research has been conducted on the lubricating mechanisms of nanoparticles, such as the protective film mechanism [13, 14], the self-repairing mechanism [15, 16], rolling friction [17, 18], and the deposition effect [19, 20]. While how nanoparticles perform under different lubricating conditions is still obscure.

At present, some research on the effect of different lubricating conditions on the lubrication performance of nanoparticles has been conducted because the previous research conditions on the mechanisms of nanoparticles are simple. Kogovsek et al. [21] investigated the influence of surface roughness and running-in on the lubrication of steel surfaces with oil containing MoS_2 nanotubes in all lubrication regimes, and experimental results showed that the lubrication behavior of MoS_2 nanotubes is not affected by surface roughness and running-in. Greenberg et al. [22] studied the effect of WS_2 nanoparticles on friction reduction in various lubrication regimes, and it was found that the addition of WS_2 nanoparticles contributes to friction reduction only in the mixed lubrication regime. Besides, the effect of nanoparticle size on the tribological performance of SiO_2 nanofluid under different lubrication conditions was evaluated, and it was indicated that different sizes of nanoparticles can respectively improve the tribological

performance of a lubricant at different experimental frequencies [23]. Furthermore, research was conducted to study the effect of sliding distance and reinforcement type on the friction and wear properties of composites [24, 25]. These studies show that different conditions have a great influence on the tribological performance of nanoparticles.

Although oil-based fluids with nanoparticles exhibit better tribological properties, the problem of environmental pollution and energy consumption should not be ignored. While water-based fluids show excellent cooling, cleaning, economy, and safety performances, which get very fast development in recent years. Despite there being a lot of studies focusing on the mechanisms of nanoparticles as lubricant additives, the research of nanoparticles under different lubrication conditions is rarely reported, including SiO_2 nanoparticles. SiO_2 nanoparticles have excellent tribological performance due to their high hardness and spherical shape [26], which has been reported in our previous work. To make up for the shortcoming of previous work, we aimed to explore the effect of surface roughness and particle size on the lubrication mechanism of SiO_2 nanoparticles in the water-based fluid.

In this paper, SiO_2 nanoparticles are evenly dispersed in water-based fluids modified by polyethylene glycol-200. A series of tests were conducted to study the influence of surface roughness on the lubrication mechanisms of SiO_2 nanoparticles while also considering the effect of load.

2. Experimental

2.1. Preparation. The reagents used in the experiments were analytical pure reagents (AR) without further treatment, and SiO_2 nanoparticles were commercially provided by a chemical reagent supplier in Shanghai, China. First, polyethylene glycol-200 (PEG-200) acts as a surfactant and was dissolved into deionized water with the help of a magnetic stirrer. Then, SiO_2 nanoparticles with a mean diameter of 30 nm were gradually dropped into the solution and stirred at 60°C for 30 min. The solution was then dispersed by an ultrasonic disperser with a frequency of 20 kHz and scattered for 5 min to ensure stabilized dispersion. The content of SiO_2 nanoparticles was 0.5 wt% and the mass ratio of nanoparticles to PEG-200 was 1:1. Afterward, certain quantities of propylene glycol, triethanolamine, polypyriloxone, boric acid, molybdenum, and so on used as lubricant additives were added into the above solution and stirred at room temperature for 20 min. Finally, a uniform and stably dispersed nanofluid was obtained, and it can be held stable for 30 days. Base fluid (with no nanoparticles) acted as a contrast sample and was prepared with the same method simultaneously. The micrograph and size distributions of SiO_2 nanoparticles dispersed in aqueous were observed by TEM (JEM-2010) and Malvern Zetasizer Nano, respectively. TEM micrograph and size distributions of SiO_2 nanoparticles were shown in Figure 1, which shows that SiO_2 nanoparticles represent a spherical shape, and the nanoparticles dispersed evenly with no apparent agglomeration in the base fluid. The size distribution illustrates that the particle size of nanoparticles has an average diameter of around 160 nm.

2.2. Tribological Tests. The tribological studies were performed using an MM-W1A pin-on-disc tester under different lubrication conditions at room temperature as per ASTM G99. The schematic diagram of the equipment is displayed in Figure 2. To study the effect of surface roughness (Ra) on the tribological performance of SiO_2 nanoparticles, the surface roughness of discs was polished with sandpaper to 0.05, 0.1, 0.3, 0.5, and 1.0 μm, respectively, before experiments. When considering the influence of load, discs with different surface roughness were performed under a load of 100, 300, or 500 N and an angular velocity of 300 rpm. Experiments lasted for a few minutes in case the original rough surface was flattened during the test. The friction coefficient is obtained, and wear scar width is measured by an electron microscope to reveal the tribological properties of SiO_2 nanoparticles. Triplicate measures were carried out for each sample, and the average date was adopted as the final experimental data.

2.3. Analysis Method. Three specimens with the sizes of 10 mm $*$ 10 mm were cut from each disc, and all the specimens were cleaned with petroleum ether before the worn surface analysis. The initial surface roughness of specimens was observed on CLSM (Olympus LEXT OLS4000) and the 3D topographies, which are shown in Figure 3. Besides, worn surface topographies and element analysis of all the specimens were analyzed with SEM (ZEISS-EVO18), and chemical states of typical elements on the worn surface were performed with XPS (LabRAM) to study the lubrication mechanisms of SiO_2 nanoparticles under different surface roughness.

3. Results and Discussion

3.1. Friction Coefficient and Wear Scar Width. The friction coefficient and wear scar width represent the lubricating properties of base fluid and nanofluid. Figure 4(a) displays the variation of friction coefficients of discs lubricated with base fluid and nanofluid under different surface roughness. No matter what the load is, the friction coefficients of both base fluid and nanofluid increase with increasing surface roughness.. Also, the friction coefficients significantly decrease when the SiO_2 nanoparticles are added into the base fluid at three different loads. Variations of wear scar widths with different surface roughness at various loads are shown in Figure 4(b). It is clear that a few upward trends of wear scar widths with surface roughness are observed. As shown in Figure 4(a) and 4(b), the addition of SiO_2 nanoparticles resulted in a significant reduction of the friction coefficient and wear scar widths at the same load. In addition, the friction coefficient and wear scar widths obtained under the base fluid and the nanofluid increased with the load. It illustrates that the surface roughness has a significant influence on the tribological performance of fluids.

The distribution characteristic of surface asperities is approximated to the sine curve, as shown in Figure 5. The height-diameter ratio (λ) was put forward to study the influence of surface roughness and particle size on lubrication

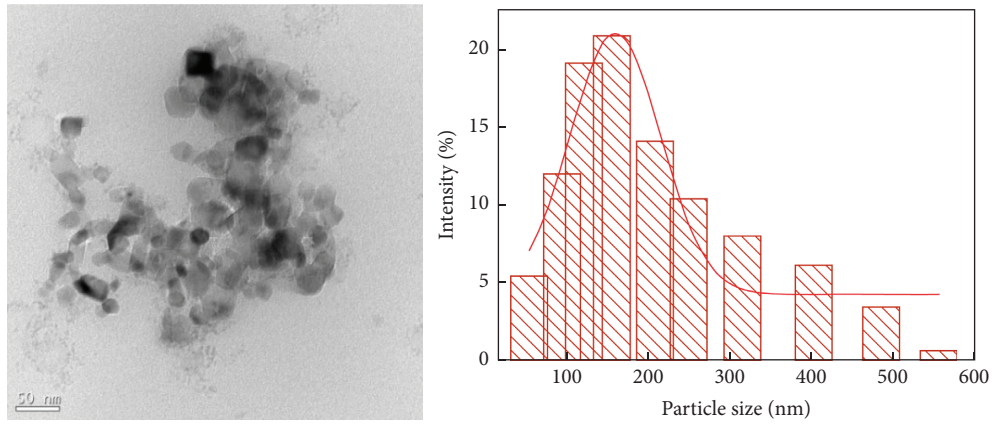

Figure 1: TEM micrograph and size distributions of SiO_2 nanoparticles.

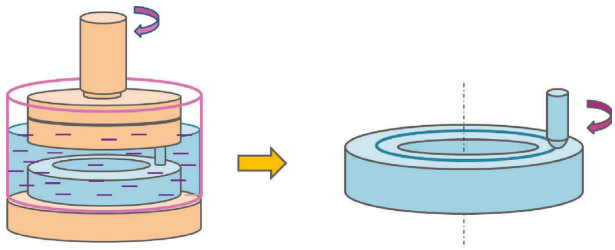

Figure 2: Schematic diagram of the pin-on-disc tester.

mechanisms of SiO_2 nanoparticles, which was calculated using the following equations:

$$Ra = \frac{H}{2} \times \frac{1}{2\pi} \int_0^{2\pi} |\sin x| \mathrm{d}x = \frac{H}{\pi} \int_0^{\pi/2} \sin x \, \mathrm{d}x = \frac{H}{\pi},$$

$$H = \pi Ra, \tag{1}$$

$$\lambda = \frac{H}{D} = \frac{\pi Ra}{D},$$

where H is the difference value between peak and valley (μm), and D is the diameter of SiO_2 nanoparticles (μm). Using the appropriate values of material properties, the calculated value of the height-diameter ratio is 1, 2, 6, 10, and 20 for Ra of 0.05–1.0 μm.

The reduction of friction coefficient and wear scar width is characterized by the lubricating performance of SiO_2 nanoparticles. To further study the influence of surface roughness and particle size on the lubricating properties of SiO_2 nanoparticles, reductions of friction coefficient of base fluid by adding SiO_2 nanoparticles under different height-diameter ratios are conducted, as shown in Figure 6(a). The reductions in friction coefficient at various loads increase first, and then decrease considerably in the range of λ from 2 to 20. Reduced friction coefficients decrease with the increasing of load when the λ is less than 6, whereas they increase with the increasing of load when λ is from 6 to 20. Besides, when the height-diameter ratio is more than 2, the influence of load on the reduction of the friction coefficient is less than that of 1 and 2. The reductions of friction coefficient reach the maximum value at λ of 2 and the minimum value at λ of 20. When the height-diameter ratio is 20, the influence of SiO_2 nanoparticles could be ignored. Figure 6(b) presents the variation curve of reductions of wear scar widths by the addition of SiO_2 nanoparticles with a height-diameter ratio. As seen in Figure 6(b), the reductions of wear scar width increase first, and then decrease, reaching the maximum value and minimum value at λ of 2 and 20, respectively. Furthermore, the reductions of wear scar width decrease with the increasing of load when λ is less than 10. On the contrary, they increase with the increasing of load when λ is 10 and 20. It's worth noting that the influence of load on the reduction of friction coefficient at λ of 1–6 is greater than that at λ of 10 and 20. When the height-diameter ratio is 20, there is almost no difference between base fluid and nanofluid. Based on the above results, it is clear that the lubricating properties of SiO_2 nanoparticles have a great relationship with surface roughness and particle size. The addition of SiO_2 nanoparticles contributes to the obvious reduction of friction coefficient and wear scar width of base fluid when the height-diameter ratio is smaller than 20, and the bigger the height-diameter ratio is, the smaller the effect of SiO_2 nanoparticles will be. Besides, the load has a great influence on the lubricating properties of SiO_2 nanoparticles when the λ is less than 10.

3.2. Worn Surface Analysis. The worn morphologies of the wear scars lubricated with base lubricant and nano-lubricant under different surface roughness are presented in Figure 7. As seen from Figures 7(a)-7(e), there are adhesion and deep scratches on the worn surface under the surface roughness of 0.05 μm. When the surface roughness increases, the worn morphologies become smoother with fewer shallow scratches. Whereas, the wear becomes severe and intensive, and deep furrows are observed in Figures 7(c)-7(e). As the surface roughness increases, the worn surface becomes rougher. Also, the effects of SiO_2 nanoparticles on worn morphologies can be clearly seen in Figures 7(f)-7(j). As seen in Figure 7(f), there are grooves and deep scratches on the worn surface, which illustrates that the addition of SiO_2 nanoparticles makes surface wear increase. While the Ra is 0.1 μm, a very smooth worn surface is obtained with nanoparticles added into the base fluid. When the surface

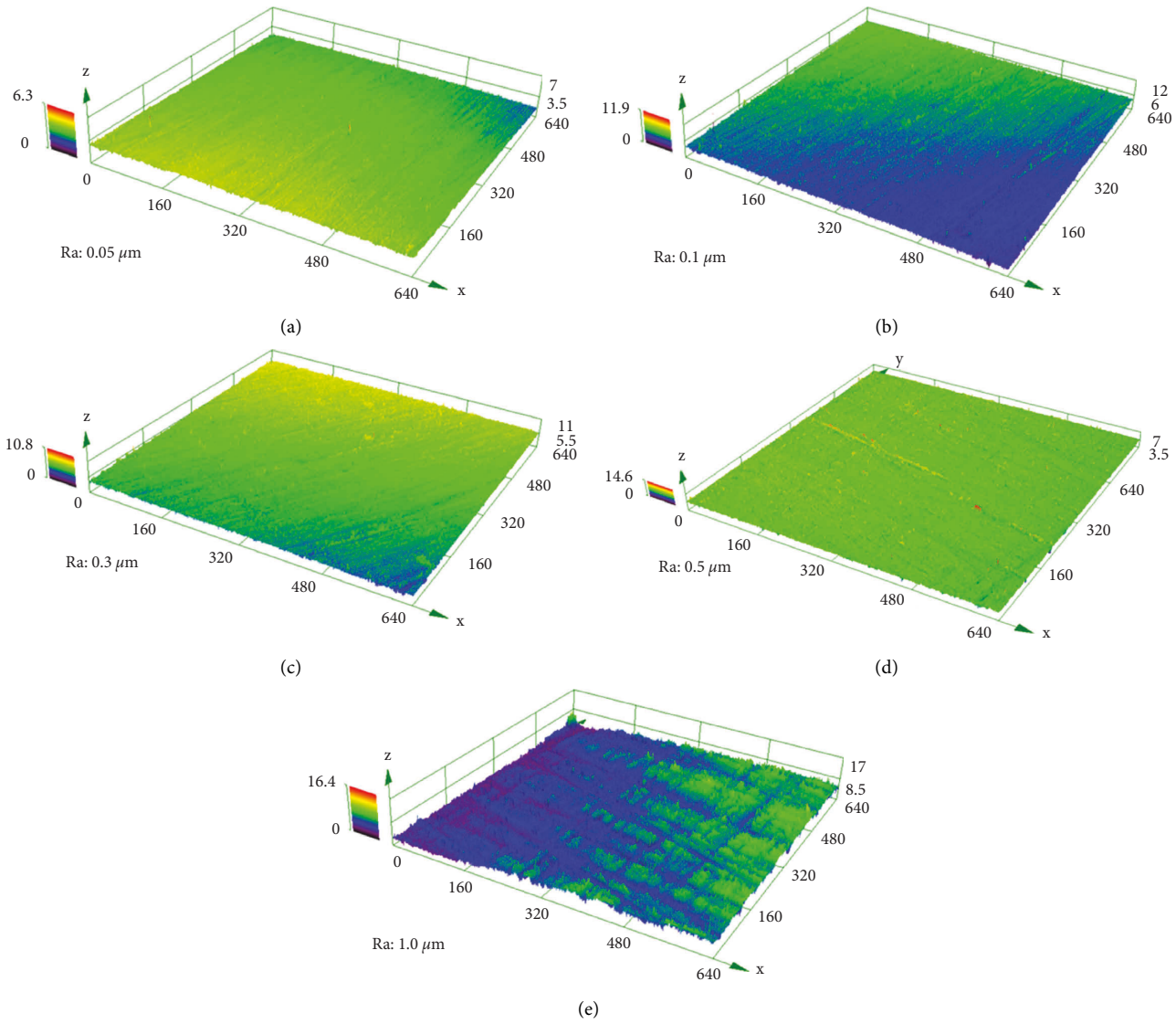

Figure 3: 3D topographies of the original surfaces.

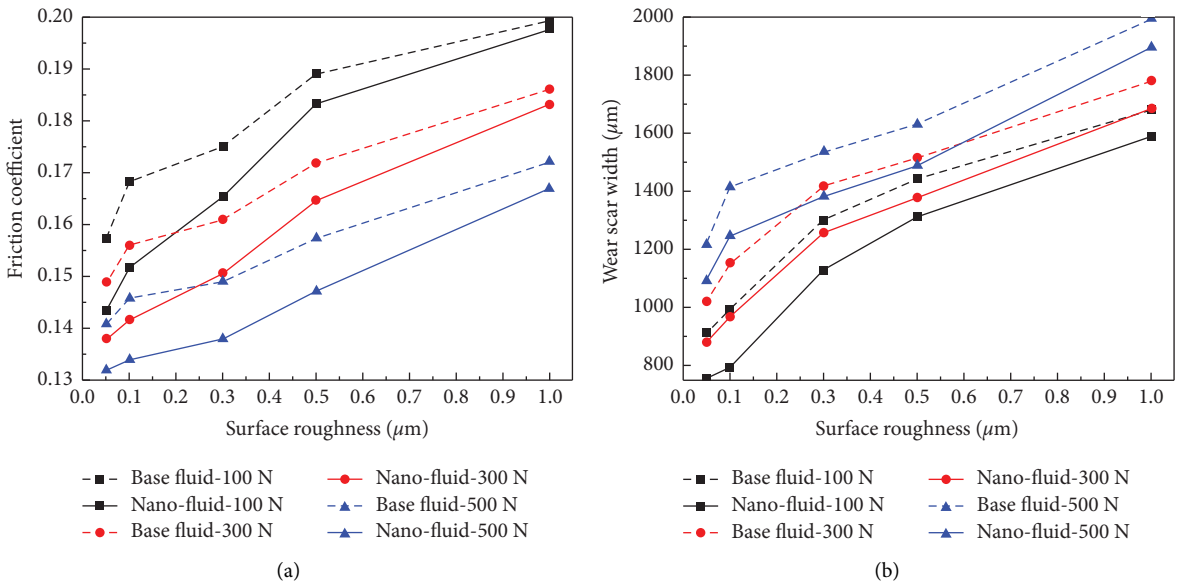

Figure 4: Variations of (a) friction coefficients and (b) wear scar widths with different surface roughness at various loads (300 rpm).

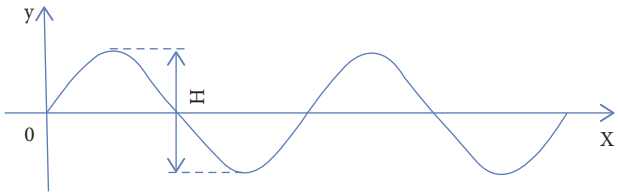

Figure 5: Distribution characteristics of surface asperities.

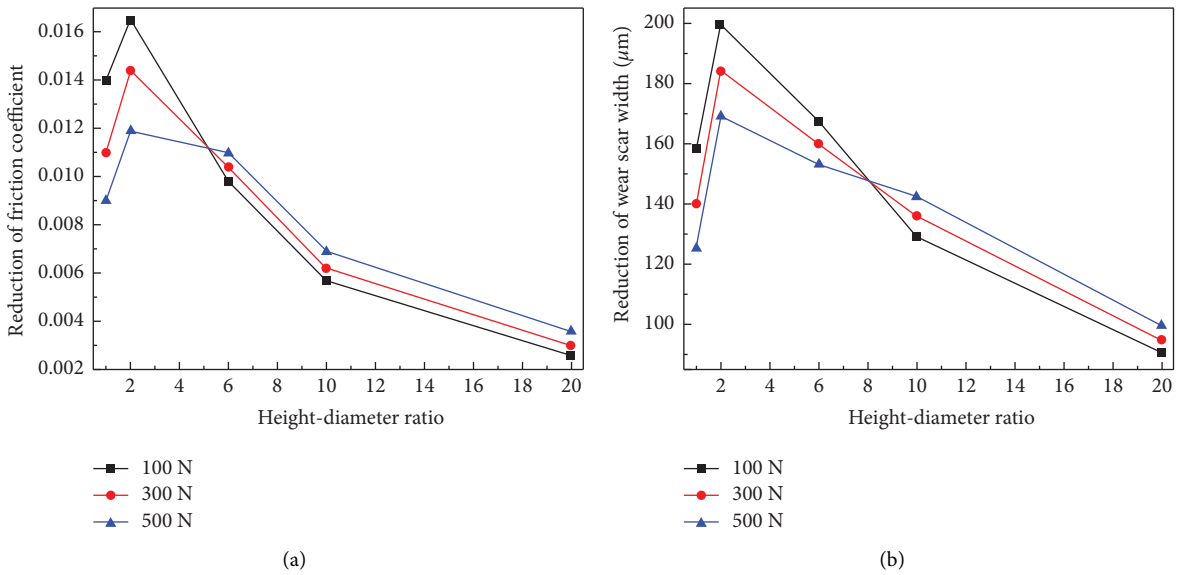

Figure 6: Reductions of (a) friction coefficients and (b) wear scar widths varied with height-diameter ratio (300 rpm).

roughness further increases to 0.3 μm, the worn surface becomes smooth after adding SiO_2 nanoparticles. When the Ra is 0.5 and 1.0 μm, there are no obvious differences between the worn morphologies under base fluid and nanofluid . These results show that surface roughness and the addition of SiO_2 nanoparticles have a remarkable influence on the worn morphology of the disc. The tribological properties that vary with the surface roughness in this study are similar to those of some researchers [27, 28], while they are different from those works, which indicated that friction is independent of surface roughness [21, 29].

The worn morphologies of the wear scars lubricated with base fluid and nanofluid under different loads are shown in Figure 8. As observed in Figures 8(a)-8(c), obvious differences between the worn morphologies are observed as the load increases when lubricated under base fluid. The worn surface becomes smooth with the increasing load, and the scratches vary from deep and dense to shallow and wide. Compared to the base fluid, the worn morphologies become considerably smoother when adding SiO_2 nanoparticles. This phenomenon shows that the increase in load makes the surface plastic deform, and the addition of nanoparticles can effectively reduce the worn rate.

3.3. Lubrication Mechanisms of SiO_2 Nanoparticles. Regardless of the effect of SiO_2 nanoparticles, the phenomenon of friction coefficients, wear scar widths, and worn morphologies under different surface roughness could be explained for the following reasons. First, it is known that the smoother the surface is, the thicker the average oil film between friction pairs will be [30], and the friction coefficient is inversely proportional to the thickness of the oil film. Besides, the slope of the rough peak is the key factor that determines the coefficient of friction, according to Ruan et al. [31], which shows an increasing trend with the increase of surface roughness. In addition, when the surface roughness is higher, surface asperities are embedded with each other, which will hinder friction pairs from sliding easily [27]. The friction of surface asperities makes the oil film break up easily, which results in the direct contact between friction pairs appearing, and then forming the abrasive wear. Therefore, it is less possible for abrasive wear to appear with the decrease of surface roughness [32]. When the surface roughness decreases to 0.05 and 0.1 μm, film lubrication is the dominant mechanism due to the thick oil film. Also, the mechanism of wear is based on the combined effect of film lubrication and abrasive wear when the Ra is 0.3 μm. When surface roughness is between 0.5 and 1.0 μm, abrasive wear is the dominant type of wear due to the thin film thickness. Based on the above reasons, the friction coefficients and wear rate increase with increasing surface roughness. When the oil film is thicker, the nanoparticles flow with the liquid, making the nanoparticles more efficient, and the nanoparticles have a good lubrication effect. When the oil film is

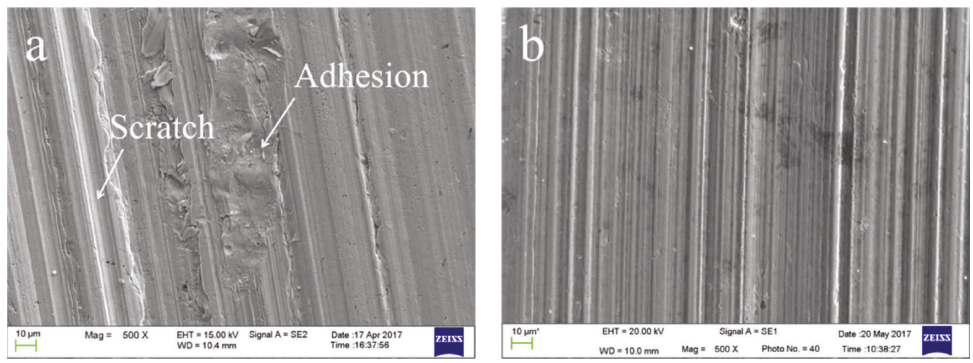

(a)

(b)

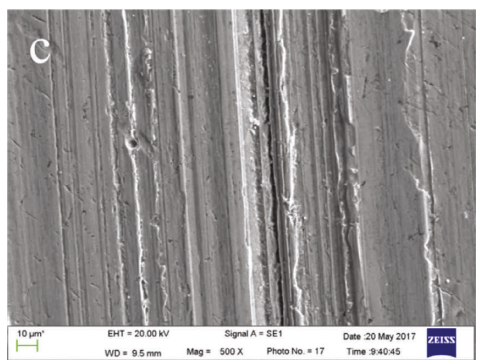

(c)

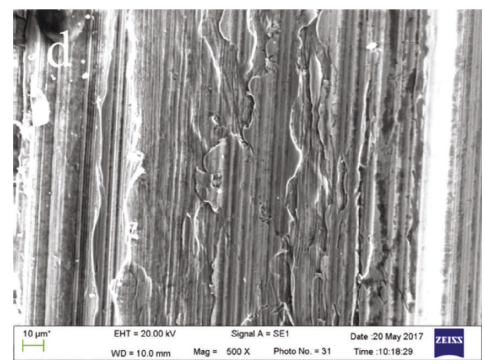

(d)

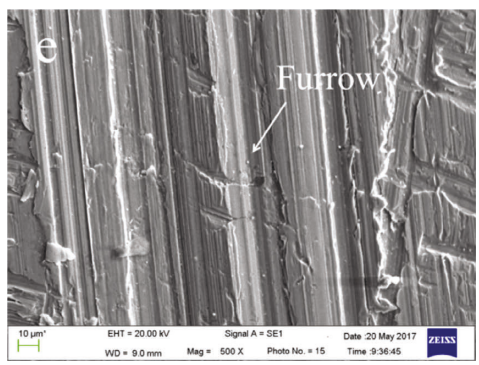

(e)

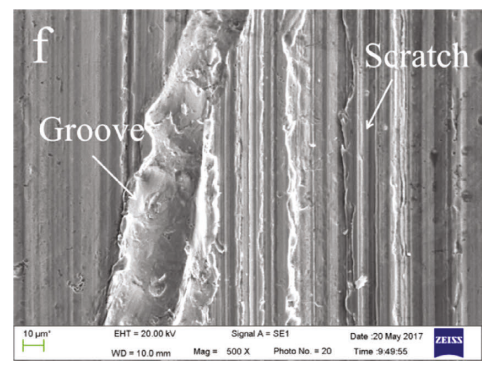

(f)

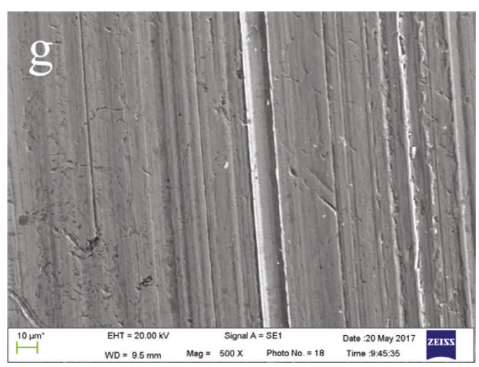

(g)

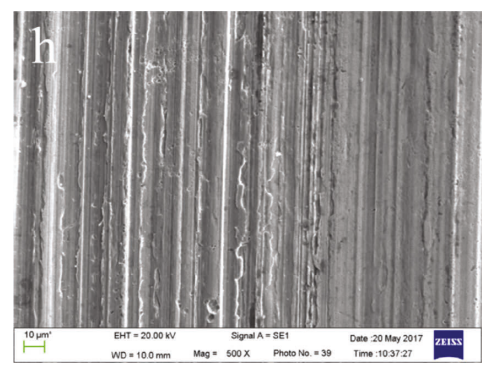

(h)

Figure 7: Continued.

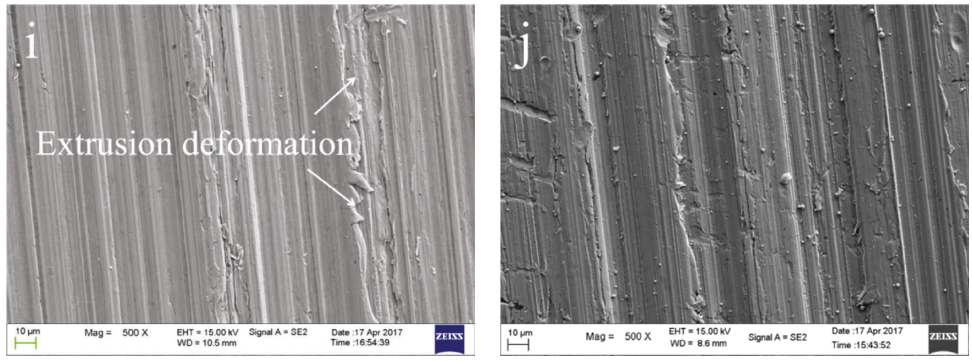

(i) (j)

Figure 7: Worn morphologies of the wear scars lubricated with base fluid (a-e) and nanofluid (f-j) under different surface roughness: (a), (f) Ra: 0.05 μm, (b), (g) Ra: 0.1 μm, (c), (h) Ra: 0.3 μm, (d), (i) Ra: 0.5 μm, (e), (j) Ra: 1.0 μm (300 (N) 300 rpm).

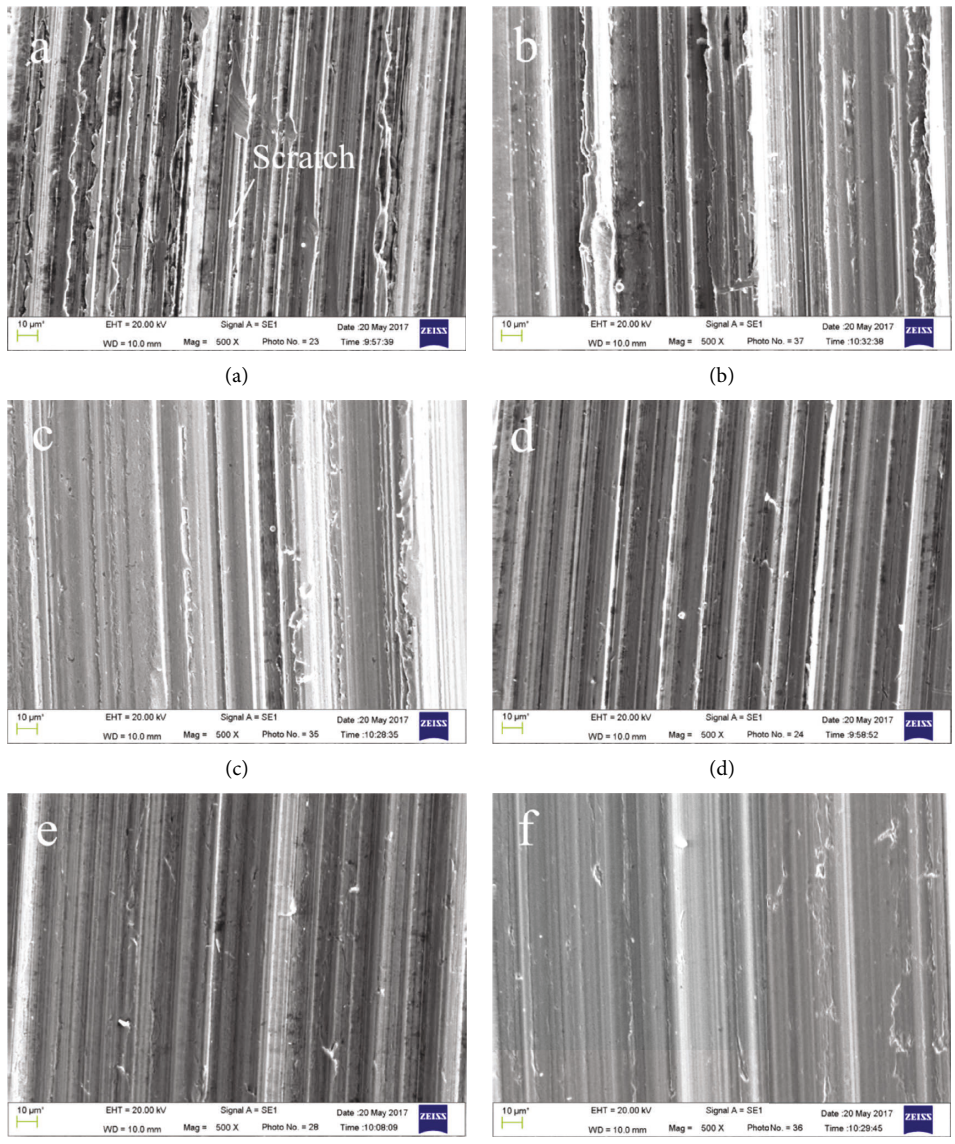

(a) (b)

(c) (d)

(e) (f)

Figure 8: Worn morphologies of the wear scars lubricated with base fluids (a), (b), (c), and nanofluid. (d), (e), and (f) under different loads: (a), (d) 100 N, (b), (e) 300 N, (c), (f) 500 N (0.1 μm, 300 rpm).

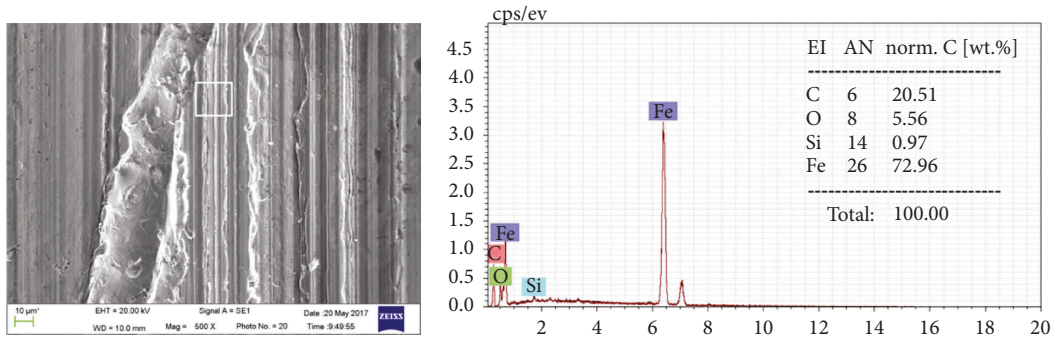

Figure 9: (a) A SEM micrograph of the wear scar lubricated with nanofluid under 300 (N) and (b) an EDS spectrum of the marked area of (a).

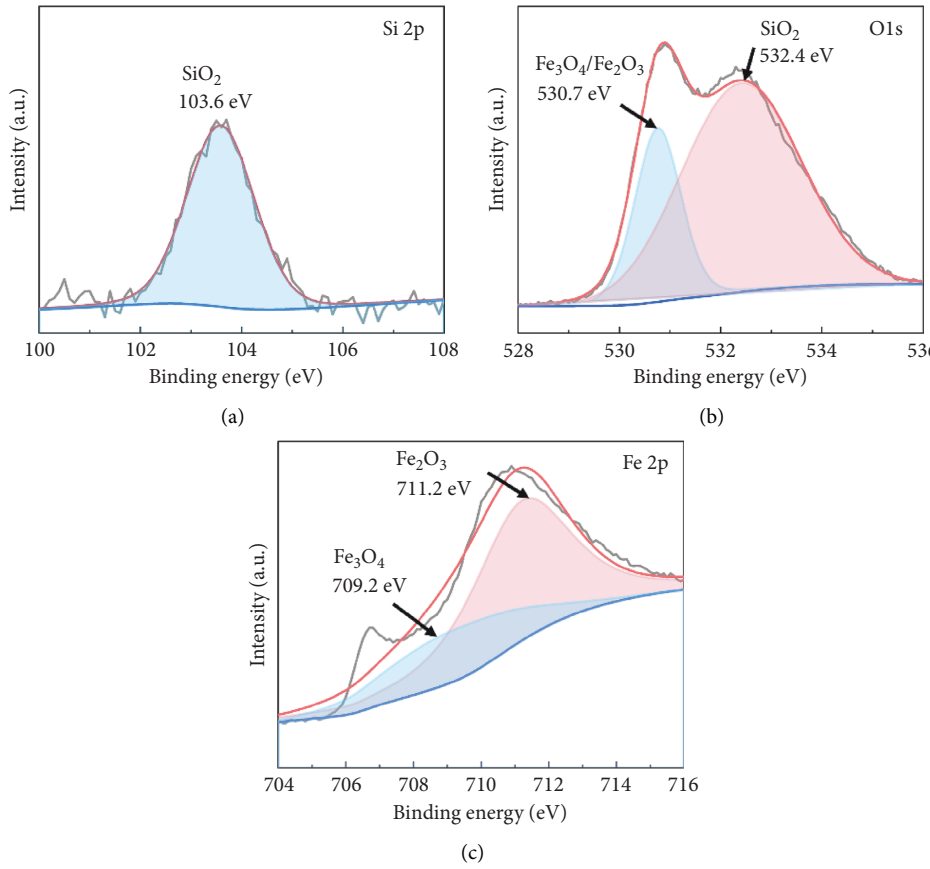

Figure 10: An XPS spectra of Si_2p, O 1s, and Fe_2p on the wear surface lubricated with 0.3 wt. % SiO_2 nanoparticles.

thin and discontinuous, the effective nanoparticles are reduced. The lubrication mechanism of SiO_2 nanoparticles in different surface roughness will be discussed later.

The phenomenon of why the effect of surface roughness on the lubricating properties of fluid varies with load could be attributed to the following aspects. Firstly, the increase in load will result in a decrease of oil film thickness [32], and the reduction of oil film thickness leads to an increase in friction coefficients and wear rates. Whereas, it's worth noting that the increase in load causes plastic deformation on the surface of the disc, making the surface asperities decrease, the actual contact area increase, and the surface become smooth. Learn from Figure 5, that the reduction of surface roughness contributes to the decrease of friction coefficients. Therefore, based on the synergetic effect of the above aspects, the friction coefficients decrease and the wear rates increase with the increase in load.

To clarify the lubrication mechanism of SiO_2 nanoparticles, an EDS analysis was conducted. Figure 9 presents the EDS spectrum of the wear scar on the disc after being

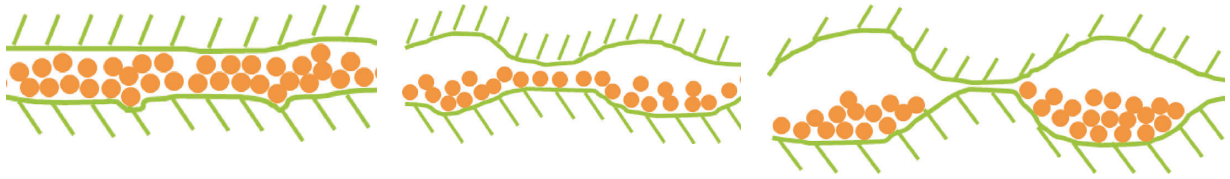

Figure 11: The lubrication mechanisms of SiO_2 nanoparticles under different height-diameter ratios (a) λ: 1, (b) λ: 6, and (c) λ: 20.

lubricated with nanofluid under 300 N. As is observed in Figure 9, there are Si and O elements on the wear scar, which illustrates that SiO_2 nanoparticles deposit on wear scars. An XPS of worn surfaces lubricated with SiO_2 nanofluid was conducted to further study the lubricating mechanisms of SiO_2 nanoparticles. The typical chemical state of element analysis results is plotted in Figure 10. Referring to the NIST Standard Reference Database 20 (version 4.1), a weak Si_2p band at about 103.6 eV [33] is associated with the O1s at 532.4 eV [34], both attributable to the Si_2p and O1s of SiO_2. The peak of O1s that emerges at 530.7 could be easily assigned to Fe_3O_4/Fe_2O_3 [35]. Moreover, two Fe_2p bands at about 709.2 eV and 711.2 eV could be identified as the Fe_2p of Fe_3O_4 [36] and Fe_2O_3 [34], respectively. It indicates that SiO_2 nanoparticles do not react with the worn surface, which plays a role in reducing friction and wear by physical action.

It is evident from Figure 4 that the addition of SiO_2 nanoparticles makes the friction coefficients and wear scar widths decrease, while not changing their variation rules as the surface roughness, load, and velocity increase. The reason could be explained by previous studies, namely that SiO_2 nanoparticles have a significant lubrication effect through rolling effect and self-repairing mechanisms [37]. While the mechanism of SiO_2 nanoparticles varies as the lubrication conditions change. The lubrication mechanisms of SiO_2 nanoparticles under three typical height-diameter ratios are given in Figure 11. As seen in Figure 11, when the height-diameter ratio is 1, the surface is so smooth that SiO_2 nanoparticles have great lubrication performance, mainly through the rolling effect. Meanwhile, SiO_2 nanoparticles will be filled into some small pits under the pressure, playing a self-repairing role due to the large actual contact area. When the height-diameter ratio increases to 6, surface roughness is significantly greater than the particle size, so SiO_2 nanoparticles have a self-repairing effect on the pits under the effect of pressure, as well as a small proportion of the rolling effect. As the roughness further increases, the effective nanoparticles decrease because of the accumulation of most of the nanoparticles in the concave peaks, making the nanoparticles almost have no lubrication effects. Therefore, the reduction of friction coefficients and wear scar widths decrease with the increase of surface roughness. In addition, learning from the grooves on the wear scar in Figure 7(e), the addition of SiO_2 nanoparticles would cause wear on the surface when the λ is 1. When the height-diameter ratio is less than 6, the increase of load has little effect on surface roughness, which merely increases the wear of the surface due to the high hardness of SiO_2 nanoparticles. When the height-diameter ratio increases to 10 and 20, the increase of load makes surface roughness decrease, which makes the self-repairing effect of nanoparticles more obvious. Therefore, the reduction of friction and wear decreases with the increase of load.

4. Conclusions

The lubrication mechanism of SiO_2 nanoparticles added to the base fluid under different surface roughness was investigated with a consideration of load and velocity. The experimental results and main findings are summarized as follows:

(1) It shows a decreasing trend of friction coefficients and wear scar widths by adding SiO_2 nanoparticles with the increase of surface roughness. When the height-diameter ratio is less than 2, SiO_2 nanoparticles obviously improve the tribological performance of base fluid, mainly due to the rolling effect mechanism. When the λ increases to 6 and 10, the self-repairing effect of SiO_2 nanoparticles is found to occur, and the rolling effect becomes less important. While there is no effect of nanoparticles on lubrication when the λ is 20, because that nanoparticle accumulated in the concave peaks, making effective nanoparticles reduce.

(2) When the height-diameter ratio is less than 6, the increase of load causes surface wear to increase because of the high hardness of SiO_2 nanoparticles. When the height-diameter ratio increases to 10 and 20, the reduction of friction and wear decreases with the increase of load because the surface roughness decreases.

Data Availability

The NIST Standard Reference Data Base 20 (version 4.1) was used for XPS analysis.

Conflicts of Interest

The authors declare that they have no conflicts of interest.

Acknowledgments

This research was funded by the Open Research Subject of the Research Center on Levee Safety Disaster Prevention, Ministry of Water Resources (LSDP202108), Fundamental

Research Funds for the Central Nonprofit Research Institutions (HKY-JBYW-2020-08), and theNatural Science Foundation of Henan Province (202300410543).

References

[1] G. Moille, L. Chang, W. Xie et al., "Dissipative ksdks-V m (laser photonics rev. 14(8)/2020)," *Laser & Photonics Reviews*, vol. 14, no. 8, Article ID 2070043, 2020.

[2] Y. Ying, B. Ma, J. Yu et al., "Whole LWIR directional thermal emission based on ENZ thin films," *Laser & Photonics Reviews*, vol. 16, no. 8, Article ID 2200018, 2022.

[3] R. Li, C. Pang, Z. Li et al., "Ultrafast s absorbers: fused silica with embedded 2D-like Ag nanoparticle monolayer: tsai spacing manipulation (laser photonics rev. 14(2)/2020)," *Laser & Photonics Reviews*, vol. 14, no. 2, Article ID 2070014, 2020.

[4] T. Liu, C. Yang, Z. Fan et al., "Spectral narrowing and enhancement of directional emission of perovskite light emitting diode by microcavity," *Laser Photonics Review*, Article ID 2200091, 2022.

[5] S. Zhao, C. Chen, W. Cai et al., "Efficiently luminescent and stable lead-free $Cs_3Cu_2C_{l5}$@Silica nanocrystals for white light-emitting diodes and communication," *Advanced Optical Materials*, vol. 9, no. 13, Article ID 2100307, 2021.

[6] H. Chen, K. Guo, J. Yin et al., "Photoluminescence-induced four-wave mixing generation in a monolayer-MoS_2-cladded GaN microdisk resonator," *Laser & Photonics Reviews*, vol. 15, no. 4, Article ID 2170023, 2021.

[7] J. Ji, Y. Bao, X. Liu, J. Zhang, and M. Xing, "Molybdenum-based heterogeneous catalysts for the control of environmental pollutants," *Ecomat*, vol. 3, no. 6, Article ID e12155, 2021.

[8] X. Xu, Y. Wang, X. Chen et al., "Semi-metal 1T' phase MoS_2 nanosheets for promoted electrocatalytic nitrogen reduction," *Ecomat*, vol. 3, no. 4, 2021.

[9] Y. Yue, H. Wang, L. Wang et al., "Direct observation of room-temperature intravalley coherent coupling processes in monolayer MoS_2," *Laser & Photonics Reviews*, vol. 16, no. 2, Article ID 2100343, 2022.

[10] S. Song, H. Shen, Y. Wang et al., "Biomedical application of graphene: from drug delivery, tumor therapy, to theranostics," *Colloids and Surfaces B: Biointerfaces*, vol. 185, Article ID 110596, 2020.

[11] S. Du, J. Sun, and P. Wu, "Preparation, characterization and lubrication performances of graphene oxide-TiO_2 nanofluid in rolling strips," *Carbon*, vol. 140, pp. 338–351, 2018.

[12] S. Xiong, B. Zhang, S. Luo, H. Wu, and Z. Zhang, "Preparation, characterization, and tribological properties of silica-nanoparticle-reinforced B-N-co-doped reduced graphene oxide as a multifunctional additive for enhanced lubrication," *Friction*, vol. 9, no. 2, pp. 239–249, 2021.

[13] C. Wang, J. Sun, C. Ge, and P. Wu, "Enhanced lubrication performance of triethanolamine functionalized reduced graphene oxide on the cold-rolled surface of strips," *Surface and Interface Analysis*, vol. 53, no. 9, pp. 762–772, 2021.

[14] J. He, J. Sun, Y. Meng, and Y. Pei, "Superior lubrication performance of MoS_2-Al_2O_3 composite nanofluid in strips hot rolling," *Journal of Manufacturing Processes*, vol. 57, pp. 312–323, 2020.

[15] J. He, J. Sun, F. Yang, Y. Meng, and W. Jiang, "Water-based Cu nanofluid as lubricant for steel hot rolling: experimental investigation and molecular dynamics simulation," *Lubrication Science*, vol. 34, no. 1, pp. 30–41, 2022.

[16] J. He, J. Sun, Y. Meng, and X. Yan, "Preliminary investigations on the tribological performance of hexagonal boron nitride nanofluids as lubricant for steel/steel friction pairs," *Surface Topography: Metrology and Properties*, vol. 7, no. 1, Article ID 015022, 2019.

[17] J. He, J. Sun, Y. Meng, H. Tang, and P. Wu, "Improved lubrication performance of MoS_2-Al_2O_3 nanofluid through interfacial tribochemistry," *Colloids and Surfaces A: Physicochemical and Engineering Aspects*, vol. 618, Article ID 126428, 2021.

[18] J. He, J. Sun, Y. Meng, Y. Pei, and P. Wu, "Synergistic lubrication effect of Al_2O_3 and MoS_2 nanoparticles confined between iron surfaces: a molecular dynamics study," *Journal of Materials Science*, vol. 56, no. 15, pp. 9227–9241, 2021.

[19] C. Wang, J. Sun, C. Ge, H. Tang, and P. Wu, "Synthesis, characterization and lubrication performance of reduced graphene oxide-Al_2O_3 nanofluid for strips cold rolling," *Colloids and Surfaces A: Physicochemical and Engineering Aspects*, vol. 637, Article ID 128204, 2022.

[20] H. Wu, J. Zhao, W. Xia et al., "A study of the tribological behaviour of TiO_2 nano-additive water-based lubricants," *Tribology International*, vol. 109, pp. 398–408, 2017.

[21] J. Kogovšek, M. Remškar, A. Mrzel, and M. Kalin, "Influence of surface roughness and running-in on the lubrication of steel surfaces with oil containing MoS_2 nanotubes in all lubrication regimes," *Tribology International*, vol. 61, pp. 40–47, 2013.

[22] R. Greenberg, G. Halperin, I. Etsion, and R. Tenne, "The effect of WS_2 nanoparticles on friction reduction in various lubrication regimes," *Tribology Letters*, vol. 17, no. 2, pp. 179–186, 2004.

[23] X. Liu, N. Xu, W. Li et al., "Exploring the effect of nanoparticle size on the tribological properties of SiO_2/polyalkylene glycol nanofluid under different lubrication conditions," *Tribology International*, vol. 109, pp. 467–472, 2017.

[24] T. Ram Prabhu, V. K. Varma, and S. Vedantam, "Effect of reinforcement type, size, and volume fraction on the tribological behavior of Fe matrix composites at high sliding speed conditions," *Wear*, vol. 309, no. 1-2, pp. 247–255, 2014.

[25] S. R. Chauhan and S. Thakur, "Effects of particle size, particle loading and sliding distance on the friction and wear properties of cenosphere particulate filled vinylester composites," *Materials & Design*, vol. 51, pp. 398–408, 2013.

[26] Y. Y. Bao, J. L. Sun, and L. H. Kong, "Tribological properties and lubricating mechanism of SiO_2 nanoparticles in water-based fluid," *IOP Conference Series: Materials Science and Engineering*, vol. 182, Article ID 012025, 2017.

[27] M. L. Rahaman, L. Zhang, M. Liu, and W. Liu, "Surface roughness effect on the friction and wear of bulk metallic glasses," *Wear*, vol. 332-333, pp. 1231–1237, 2015.

[28] S. F. Tian, L. T. Jiang, Q. Guo, and G. H. Wu, "Effect of surface roughness on tribological properties of TiB_2/Al composites," *Materials & Design*, vol. 53, pp. 129–136, 2014.

[29] P. L. Menezes, Kishore, and S. V. Kailas, "Influence of surface texture and roughness parameters on friction and transfer layer formation during sliding of aluminium pin on steel plate," *Wear*, vol. 267, no. 9-10, pp. 1534–1549, 2009.

[30] L. S. H. Chow and H. S. Cheng, "The effect of surface roughness on the average film thickness between lubricated rollers," *Journal of Lubrication Technology*, vol. 98, pp. 117–124, 1976.

[31] J. Ruan and B. Bhushan, "Atomic-scale and microscale friction studies of graphite and diamond using friction force microscopy," *Journal of Applied Physics*, vol. 76, no. 9, pp. 5022–5035, 1994.

[32] H. Chen, A. Namura, M. Ishida, and T. Nakahara, "Influence of axle load on wheel/rail adhesion under wet conditions in consideration of running speed and surface roughness," *Wear*, vol. 366-367, pp. 303–309, 2016.

[33] Th. Gross, M. Ramm, H. Sonntag, W. Unger, H. M. Weijers, and E. H. Adem, "An XPS analysis of different SiO_2 modifications employing a C 1s as well as an Au 4f7/2 static charge reference," *Surface and Interface Analysis*, vol. 18, no. 1, pp. 59–64, 1992.

[34] B. J. Tan, K. J. Klabunde, and P. M. A. Sherwood, "X-ray photoelectron spectroscopy studies of solvated metal atom dispersed catalysts. Monometallic iron and bimetallic iron-cobalt particles on alumina," *Chemistry of Materials*, vol. 2, pp. 186–191, 1990.

[35] E. Paparazzo, "XPS and auger spectroscopy studies on mixtures of the oxides SiO_2, Al_2O_3, Fe_2O_3 and Cr_2O_3," *Journal of Electron Spectroscopy and Related Phenomena*, vol. 43, no. 2, pp. 97–112, 1987.

[36] P. Marcus and J. M. Grimal, "The antagonistic roles of chromium and sulphur in the passivation of Ni, Cr, Fe alloys studied by XPS and radiochemical techniques," *Corrosion Science*, vol. 31, pp. 377–382, 1990.

[37] Y. Bao, J. Sun, and L. Kong, "Effects of nano-SiO_2 as water-based lubricant additive on surface qualities of strips after hot rolling," *Tribology International*, vol. 114, pp. 257–263, 2017.